Penerbit Akademia Baru

Journal of Advanced Research in Fluid Mechanics and Thermal Sciences

Journal homepage: www.akademiabaru.com/arfmts.html
ISSN: 2289-7879

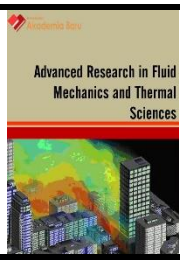

Enhancement of Wind Farm Power Density by an Oblique Linear Configuration

Open Access

Ahmad Zakaria[1,*], Mohd Shahrul Nizam Ibrahim[1]

[1] Numerical Simulation Lab, Universiti Kuala Lumpur Malaysia Italy Design Institute, 56100 Kuala Lumpur, Wilayah Persekutuan Kuala Lumpur, Malaysia

ARTICLE INFO

Article history:
Received 31 December 2019
Received in revised form 6 February 2020
Accepted 6 February 2020
Available online 24 April 2020

Keywords:
CFD analysis; turbine interaction; power density; wind farm

ABSTRACT

An optimum layout of turbines in a wind farm can be measured by a parameter called wind power density. This is essentially the power generated by the turbine per unit area. This paper attempts to demonstrate how the parameter could be increased by an oblique array configuration. In this numerical study, multiple helical Savonius turbines were used to compare the performances of different wind farm layout designs by using a finite element CFD solver. The optimum spacing between turbines was first determined for three turbine array configurations. It was then extended to a nine-turbine array in V formation. Three wind farm configurations were considered namely all in clockwise (CW) or counterclockwise direction (CCW) and the other is a combination of CW and CCW direction. The wind power density for each configuration was then compared. The nine turbines arranged in V formation has improved its power density by 4 to 5 times when compared to nine isolated turbines in a wind farm.

1. Introduction

One of the important criteria in a wind farm design is an improved average power output resulted from interflow interactions between individual turbines. Generally, this can be achieved by computing the power coefficient of the individual turbine within the wind farm and compare to an isolated turbine of similar design.

Whittlesey *et al*., [1] proposed the array performance coefficient, C_{AP} in order to determine the effectiveness of the turbine array. For C_{AP} value of below 1, it indicates the array does not perform in a positive way hence the decline in the overall performance. On the contrary, for C_{AP} more than 1 it shows a good interaction between the turbines in the arrays, hence improves the overall performance. They also defined wind farm power density, C_{PD} parameter as

* *Corresponding author.*
E-mail address: dzakaria@unikl.edu.my (Ahmad Zakaria)

https://doi.org/10.37934/arfmts.70.1.7788

$$C_{PD} = K.C_{AP}\frac{A_{iso}}{A_{array}} \quad (1)$$

where K is the number of turbines, A_{iso} is the area occupied by an isolated turbine and A_{array} is the area of the wind farm.

While others [2,3] simply define wind farm power density as the total power generated per unit area (watt/m^2).

As far as Savonius turbines are concerned, the power enhancement hence an increase in power density is a result of a coupling effect attributed to flow interaction between individual turbines [4]. In addition, an experimental investigation by Shigetomi *et al*., [5] revealed that it is also caused by the Magnus effect. While the increase in power is dependent on certain parameters such as gap distance and relative angular position with respect to the upstream turbine [6], relative phase angle [4] and turbine angular direction [7], configuration design also plays an important role to ensure maximum power output.

Linear array configuration implies the placement of the turbines in a right angle to the flow stream [8]. Mereu *et al*., [9] introduced the term β as wind incidence angle into linear array analysis to vary the wind direction applied to the system. In a similar manner [6], the term parallel configuration is used to demonstrate the placement of the turbine next to each other at the right angle to streamline. If the downstream turbine is located at an angle relative to either advancing or returning blade of the upstream turbine, this is called an oblique configuration or array. This concept can further extend to a linear oblique array [10]. A three-turbine arranged in a triangular formation can further be divided into either forward or backward oblique configurations [11]. The forward configuration consists of two upstream turbines and one downstream turbine while backward configuration developed with one upstream turbine and two downstream turbines. Finally, a clustered wind farm may consist of two or more patterns of specific configuration in a given area [12,13]. Examples of published wind farm configurations are illustrated in Figure 1.

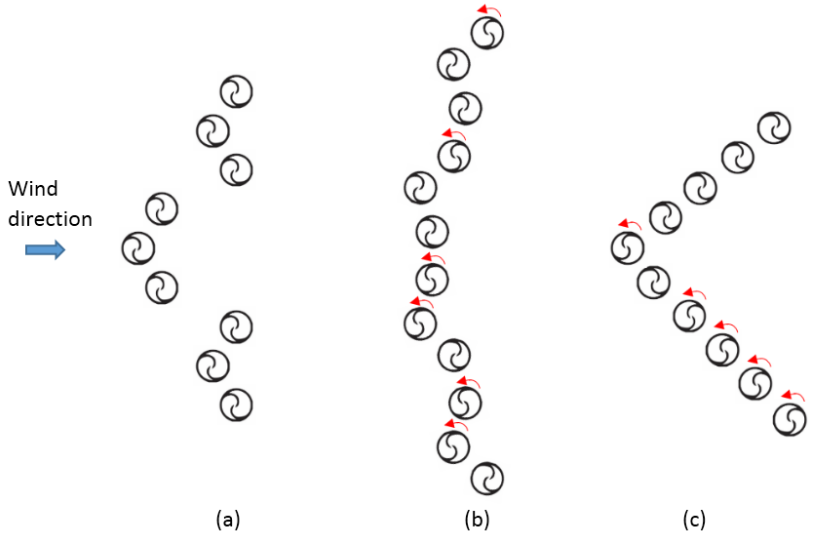

Fig. 1. Wind farm layout of Savonius turbines in different configurations (a) Shaheen *et al*., [12] (b) Zheng *et al*., [13] (c) Ibrahim and Elbaz [2]

A previous study by Ahmed and Ahmed [2] used ten turbines placed in V-formation improved the overall turbine performance by 40% compared to an isolated turbine. Extended version [2] of thirty turbines arranged in 3 big clusters shows the power density of the present wind farm design 5 times

higher than a farm consists of the same number of turbines placed far apart. A similar framework of a study employing a combination of Savonius turbine configuration is developed by Mohammed Shaheen *et al.,* [6,12]. They found that the power density of 27 turbine farm is 4 times higher than 27 isolated turbine farms. Another study on Darrieus shows the improvement of power density by 13 for nine Darrieus turbine farms [14]. The placement of the turbine in a specific pattern and configuration helps to maximize the power generation in limited wind farm space.

Variation in the gap distance which is usually defined per unit diameter and turbine relative angle has been investigated by many researchers in an attempt to optimize the overall turbine layout. The best configuration shows an improvement of 34% of the overall power efficiency [6]. Several configurations involving two and three turbines in parallel, oblique and triangle configurations were evaluated using computational fluid dynamics simulations. The optimum gap distance is between 0.1 to 1Diameter. Later work by [11] is reported to have obtained similar results. Other investigations to find optimal gap distance include [15,16]. By defining constraints in terms three velocity regions for unsteady flow generated by a turbine, Zhang *et al*., [10] then applied the swarm particle optimization algorithm for optimal turbine layout. Again, an improvement of 23% was obtained.

The present study focuses on the development of oblique linear configuration by investigating the effect of the gap distance for three turbines located either at the advancing region or reducing region of the upstream turbine. The optimum gap distance obtained from both scenarios is then used to develop a wind farm comprising of nine helical Savonius turbines. The analysis is based on a commercial finite element method based CFD solver, Acusolve.

2. Turbine Performance

The no-load condition is normally assumed to predict the turbine performance at a wind speed of interest (V) using CFD. The power of a turbine is computed by knowing torque and rotational speed (ω). The power efficiency, C_p is defined as the ratio of generated power to the power available in the environment.

$$C_p = \frac{\tau\omega}{0.5\rho A V^3} \tag{2}$$

where τ is predicted turbine torque via CFD (N.m), ρ is the air density, and A is turbine swept area (m^2). The optimum turbine tip speed ratio is firstly obtained based on the power coefficient versus tip speed ratio curve which employs the turbine rotational speed into the CFD analysis based on TSR relation as shown in Eq. (3),

$$TSR = \frac{\omega R}{V} \tag{3}$$

where R is the turbine radius.

The power density is then calculated based on the overall performance of the present configuration and compared to the nine isolated turbines. Power density is defined as the total power generated by farm per unit wind farm area occupied by the wind turbines. The wind farm power density, PD is measured based on Eq. (4).

$$PD = \frac{Power\ output\ of\ farm}{Area\ of\ farm} \tag{4}$$

3. Material and Method

Three-dimensional (3D) simulation of the Savonius turbine was adopted in this study. The configuration of the turbine is summarized in Table 1 and Figure 2.

Table 1
Helical Savonius wind turbine modeling data

Turbine Parameter	Description
Turbine type	Helical Savonius
Turbine height, H	0.5 m
Turbine diameter, D	0.27 m
Blade twist angle	90°
Overlap ratio (e/d)	0.242

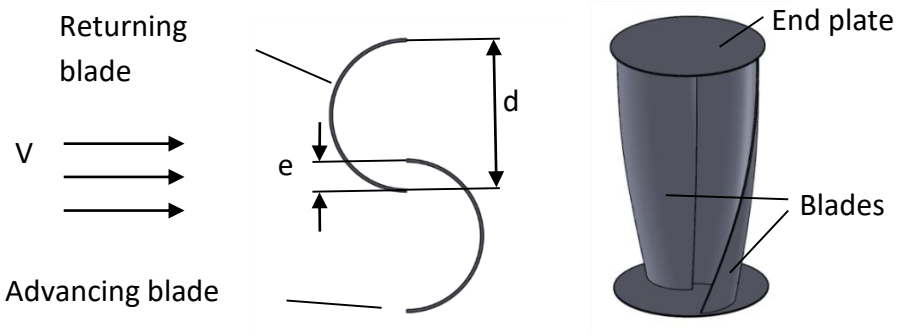

Fig. 2. Parameter annotation of Savonius wind turbine

A 3D computational domain with a dimension of x = 30D, y = 16D and z = 16D [17] is divided into two sub-domains (Domain I and Domain II) to demonstrate the flow around the Savonius turbine as shown in Figure 3. The turbine is placed at the center of the domain. The boundary condition of the present CFD analysis as summarized in Table 2.

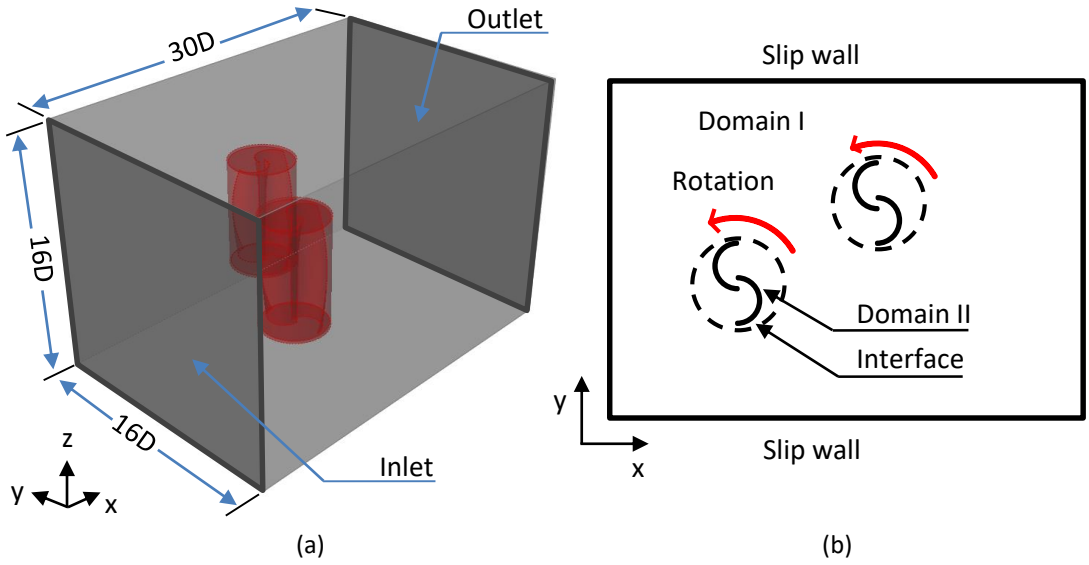

Fig. 3. (a) CFD domain (b) 2D view of CFD analysis domains

Table 2
Helical Savonius wind turbine modeling data

Boundary condition	Description
Inlet	5 m/s wind speed along the x-direction
Outlet	Atmospheric pressure
Slip	Slip condition on other domain walls
No slip	Assigned on the rotor surface
Interface	The overlap surface between two sub-domains is assigned as an interface with no boundary condition

Initially, the analysis was performed on an isolated turbine and then followed by two and three turbines in the oblique configuration. Finally, the parameters obtained are used in the evaluation of wind farm configurations.

3.1 Oblique Two Turbines Configuration

The oblique two turbine configuration consists of two turbines placed 60^o relative to each other. This is the optimum relative distance found by Mohammed Shaheen [6] for an oblique two turbines configuration. The present analysis is divided into two cases as shown in Figure 4. Case I employs turbine #2 at 60^o below the streamline while Case II employs the placement of downstream turbine 60^o above the streamline. Both turbines are set to rotate in counter-clockwise (CCW). The optimum tip speed ratio used throughout this investigation.

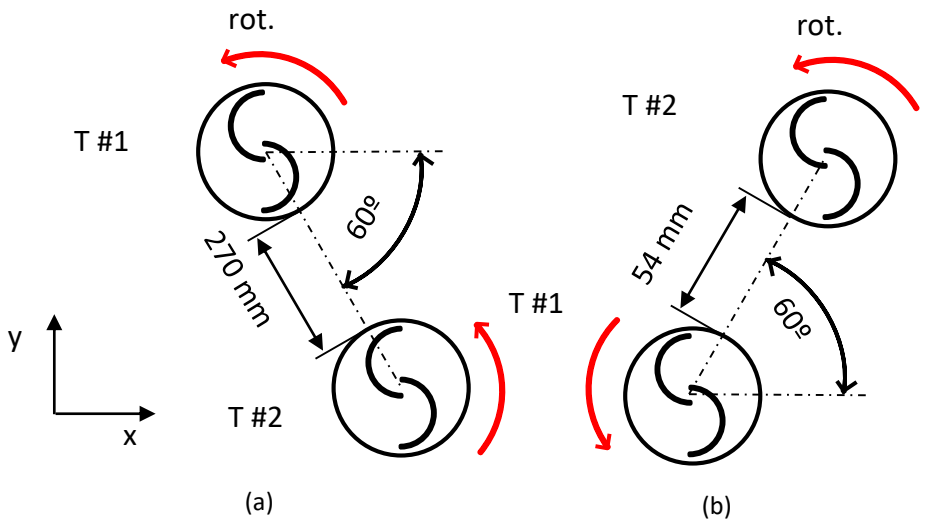

Fig. 4. Oblique two turbines: 2D view (a) Case I – 1Diameter gap = 270mm (b) Case II- 0.2Diameter of gap distance = 54mm [6]

In Case III, the downstream turbine (turbine #2) is set to rotate in the opposite direction of turbine #1. The analysis was then repeated by varying the gap distance between the turbines. Table 3 shows the gap distance variation used in this study.

Table 3
Gap distance study

Gap distance, S	Description
0.2 Diameter	The placement coordinate of the consecutive turbine with respect to turbine diameter
0.5 Diameter	
1.0 Diameter	
1.5 Diameter	
2.0 Diameter	

3.2 Oblique Three Turbine Configuration

This is an extension of the oblique two turbines described in 3.1. Turbine #3 is placed at a gap distance from the turbine #2. Three cases of oblique three configurations are defined as in Figure 5. The gap distance between turbines is varied according to Table 3. All turbines are set to rotate in CCW in case I and case II. However, for the case III, the upstream turbine is set to rotate in CCW and the turbine #2 and turbine #3 are set in CW direction. The turbine relative angle, α is kept constant for each case while varying the gap distance between the turbines.

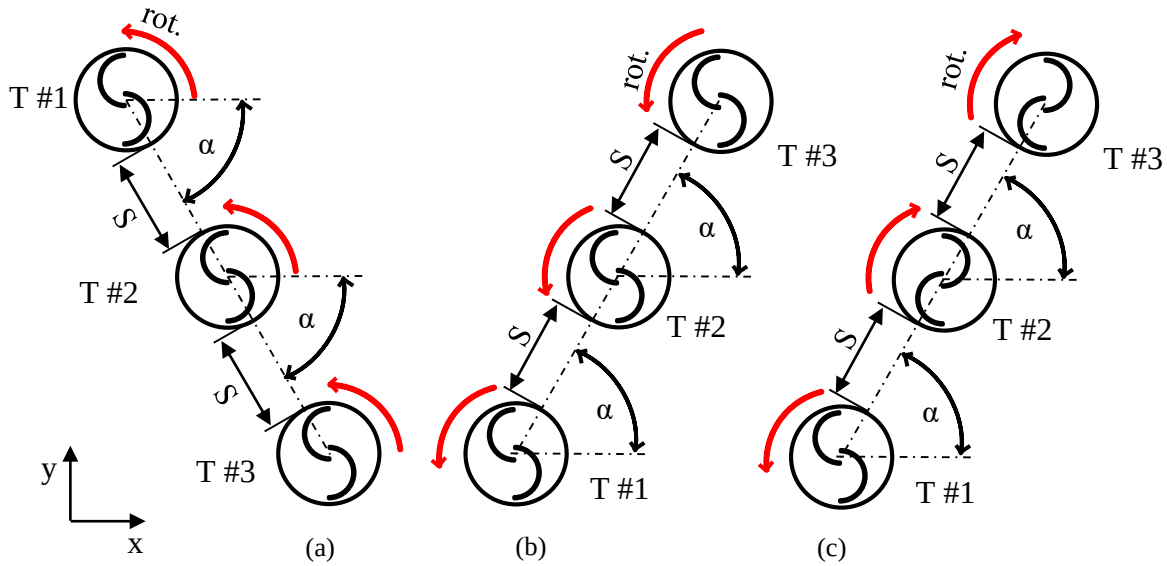

Fig. 5. Configuration of three turbines (a) Case I: α = -60° (b) Case II: (c) Case III: α = +60° Counter rotation configuration

4. Results and Discussion

The main objective of the above exercise was to determine an optimum distance at 60^o angle so that maximum power can be achieved by overall turbine performance. The published configuration was validated numerically and applied to the present study.

4.1 Wake Behind an Isolated Turbine

The performance evaluation of the isolated turbine shows that its power coefficient of 0.128 was achieved at the tip speed ratio of 0.7 [18]. Figure 6(a) shows the wake structure behind the isolated turbine at a wind speed of 5 m/s. It clearly shows vortices formed outside the wake region and low-velocity region inside the wake. The position of the strong vortex at the advancing blade appeared to

be the same as captured by PIV [19]. The initial flow velocity recovered at 7Diameter distance downstream. In order to ease the comparison between a farm comprising isolated turbines, the layout of nine turbines is shown in Figure 6(b) was proposed.

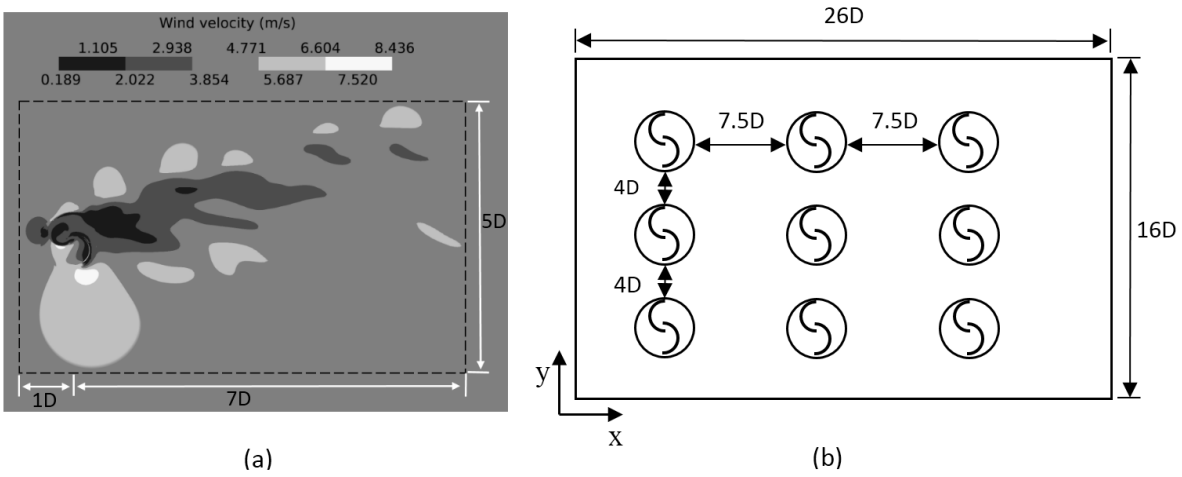

Fig. 6. (a) Flow separation color by velocity data (b) Nine isolated turbine configuration

Each turbine is placed outside the wake region of the nearest turbines. Thus, the placement of nine isolated turbines occupies an area of 6.3 m^2. Based on Eq. (4), the power density of nine isolated helical Savonius turbines is 2.38 watt/m^2.

4.2 Oblique Two Turbine Layout

Table 4 shows the results of the oblique two turbines at the optimum gap distance for Case I and Case II [6].

Table 4
Oblique two turbines at gap distance of 1Diameter and 0.2Diameter respectively

Case	Power efficiency, C_p	Turbine rotation	Description
I	Turbine #1 = 0.124 Turbine #2 = 0.134	Co-rotating (CCW)	Overall turbine performance improves by 4%
II	Turbine #1 = 0.130 Turbine #2 = 0.120	Co-rotating (CCW)	Overall turbine performance reduces by 8%

The result for Case I shows a close agreement with published data in [6] while Case II shows a reduction in the overall turbine performance as helical turbine used in the present study. The oblique two configuration Case III was then performed to obtain optimum distance for counter-rotating conditions. Only the configuration of turbine #2 above the streamline was considered at this stage. Figure 7 shows the turbine performance data for oblique two turbines configuration for Case III. The turbine's overall performance increases as the gap distance is increased. For a gap distance of more than 1Diameter, the increased power coefficient is not significant (2% to 3% higher). Thus, the gap distance of 1Diameter is good enough to obtain high overall power performance. The adaptation of 1Diameter gap distance for the counter-rotation direction shows a similar performance to the isolated turbine.

4.3 Three Turbine in Oblique Configuration

Figure 8 to Figure 10 shows the turbine performance of individual turbines at different gap distances for the three cases respectively. The 1Diameter gap distance shows better improvement for Case I and Case III. The overall turbine performance improved by 5% and 2% respectively. For Case II, the gap distance of 0.5Diameter shows the highest overall turbine performance. The turbine performance improved by 10%. Figure 8 also revealed that as the gap distance increased further than 1Diameter, the turbines tend to behave like an isolated turbine.

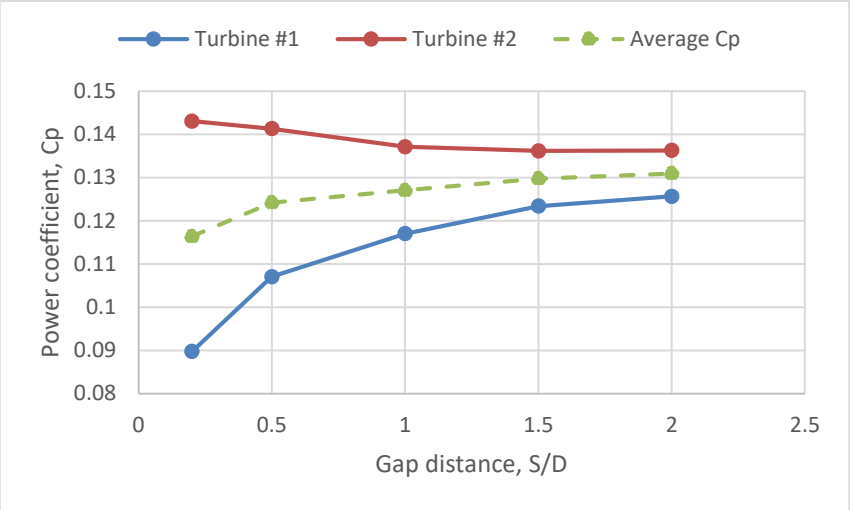

Fig. 7. Counter rotation analysis for oblique two turbines configuration (Case III)

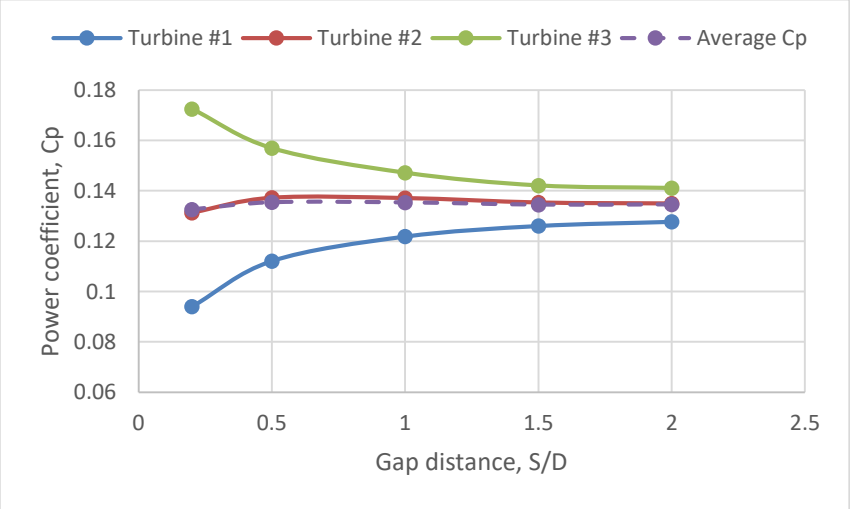

Fig. 8. Oblique three turbine performance data (Case I)

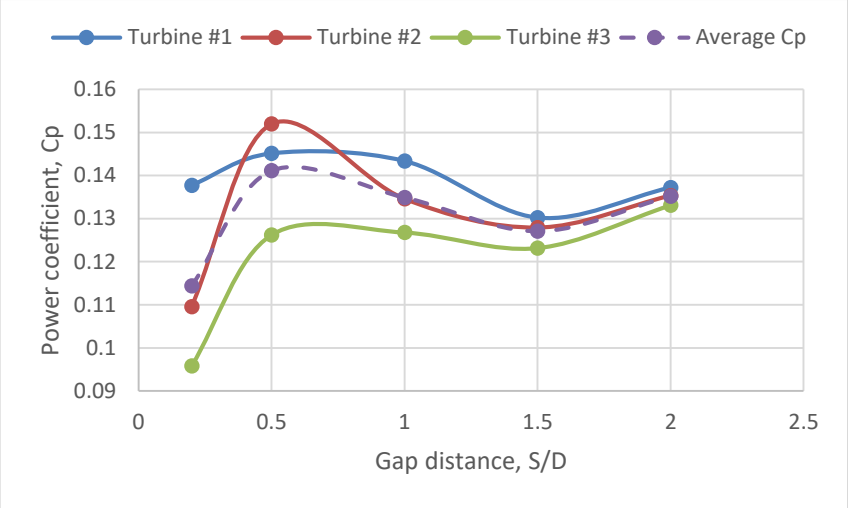

Fig. 9. Oblique three turbine performance data (Case II)

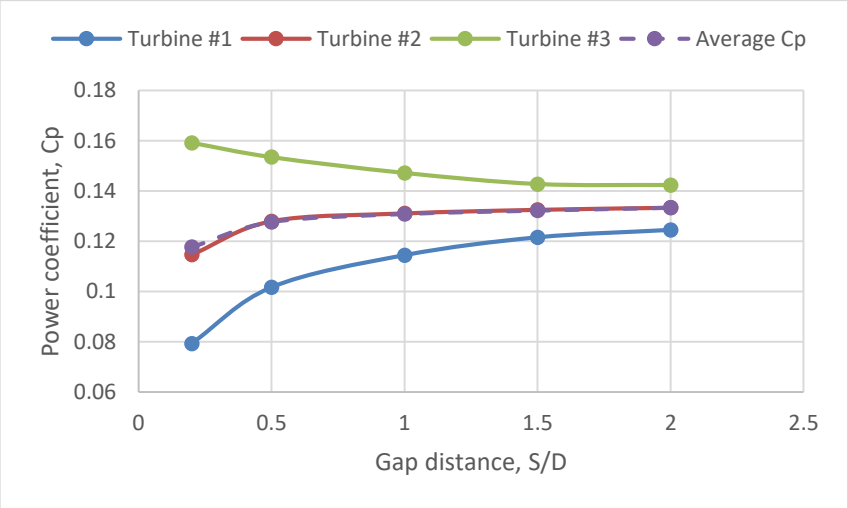

Fig. 10. Oblique three turbine performance data (Case III)

4.4 Wind Farm Performance

Wind farm comprising nine turbines (Wind farm A) was developed based on the finding in the previous section. In this study, the nine turbines were arranged in V- formation based on Case I and Case II results. All turbines above the streamline were placed at 0.5Diameter gap distance while the turbines under the streamline were placed at 1Diameter gap distance. The individual turbine performance is shown in Figure 11. The performance of the turbine on the upper side with 0.5Diameter gap distance shows a reduction in the performance while on the lower side with 1Diameter gap distance shows nearly constant improvement. Figure 12 shows the formation of strong tip vortices (red contour) near the advancing blades of turbines below the mainstream. This phenomenon happens when the reverse flow combines with the upstream flow and thus creating high speed and low pressure regions [20]. Table 5 shows the power density compared with the published data of the same configuration.

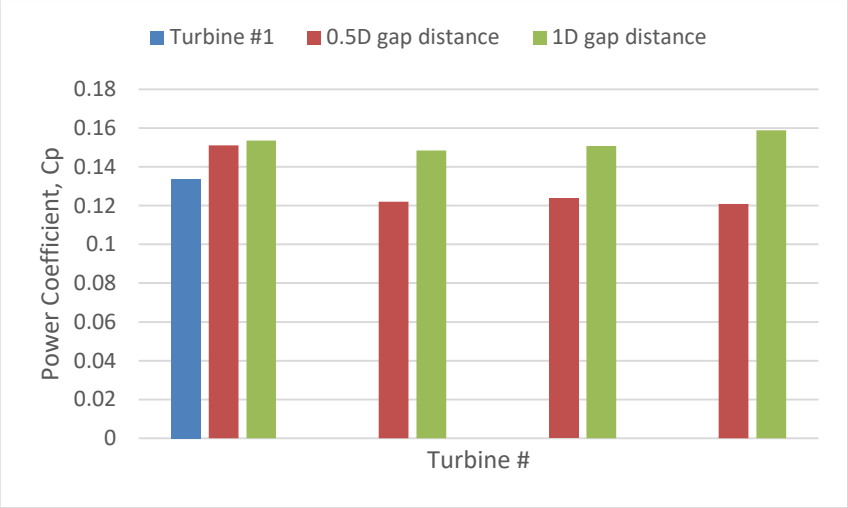

Fig. 11. V-formation wind farm performance data (Wind Farm A)

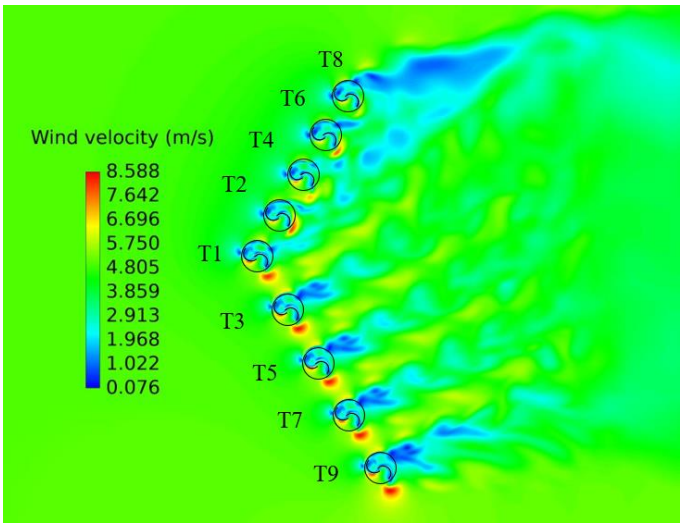

Fig. 12. Wake generated by V-formation wind farm (Wind Farm A)

Table 5
Wind farm power density

Wind farm	Total Power (watt)	Power density (watt/m^2)	Turbine configuration description
A	13.06	11.94	All turbine in CCW rotation direction
B	12.98	10.47	All turbine in CCW rotation direction [18]
C	13.24	10.68	The turbine at returning blade of the upstream turbine is allowed to rotate in CW while the rest are in CCW [18]
Isolated nine turbines	12.56	2.38	The wind turbine is placed outside the wake region of the isolated turbine

The nine wind farm configuration A, B and C show power density improvement by 4 to 5 times higher than the nine isolated turbines. Even though the wind farm A configuration shows the highest power density, the total power generated was lower than wind farm C which employs counter-rotation behavior in the farm configuration. Wind farm C configuration generates 1.4% total power over wind farm A. Thus, the selection of wind farm C configuration can be considered to the actual fabrication and field testing.

5. Conclusions

With the appropriate gap distance, the oblique turbine configuration demonstrates a greater interaction between neighbouring turbines, hence an increase in the overall turbine performance. The arrangement of the turbine in the oblique configuration shows that the overall power increases with the number of turbines in the array. In addition, the result also indicates, the placement of downstream turbines in 60^{o} at the advancing region can yield a better performance improvement in both oblique two turbines and oblique three turbines. The present study also confirmed that wind farm power density is highly dependent on the gap distance. The wind farm of nine turbines power density shows improvement up to 5 times higher than isolated nine helical turbines.

Acknowledgment

The authors would like to acknowledge the Malaysian Electricity Supply Industries Trust Account (MESITA) through the Ministry of Energy, Science, Technology, Environment & Climate Change (MESTECC) for funding this research.

References

[1] Whittlesey, Robert W., Sebastian Liska, and John O. Dabiri. "Fish schooling as a basis for vertical axis wind turbine farm design." *Bioinspiration & Biomimetics* 5, no. 3 (2010): 035005. https://doi.org/10.1088/1748-3182/5/3/035005

[2] Ibrahim, Ahmed, and Ahmed MR Elbaz. "Investigating Efficient Clusters of Savonius Wind Turbines." In *ASME Turbo Expo 2018: Turbomachinery Technical Conference and Exposition*. American Society of Mechanical Engineers Digital Collection, 2018. https://doi.org/10.1115/GT2018-75405

[3] Hezaveh, Seyed Hossein, Elie Bou-Zeid, John Dabiri, Matthias Kinzel, Gerard Cortina, and Luigi Martinelli. "Increasing the power production of vertical-axis wind-turbine farms using synergistic clustering." *Boundary-Layer Meteorology* 169, no. 2 (2018): 275-296. https://doi.org/10.1007/s10546-018-0368-0

[4] Sun, Xiaojing, Daihai Luo, Diangui Huang, and Guoqing Wu. "Numerical study on coupling effects among multiple Savonius turbines." *Journal of Renewable and Sustainable Energy* 4, no. 5 (2012): 053107. https://doi.org/10.1063/1.4754438

[5] Shigetomi, Akinari, Yuichi Murai, Yuji Tasaka, and Yasushi Takeda. "Interactive flow field around two Savonius turbines." *Renewable Energy* 36, no. 2 (2011): 536-545. https://doi.org/10.1016/j.renene.2010.06.036

[6] Shaheen, Mohammed, Mohamed El-Sayed, and Shaaban Abdallah. "Numerical study of two-bucket Savonius wind turbine cluster." *Journal of Wind Engineering and Industrial Aerodynamics* 137 (2015): 78-89. https://doi.org/10.1016/j.jweia.2014.12.002

[7] Jang, Choon-Man, Young-Gun Kim, Sang-Kyun Kang, and Jang-Ho Lee. "An experiment for the effects of the distance and rotational direction of two neighboring vertical Savonius blades." *International Journal of Energy Research* 40, no. 5 (2016): 632-638. https://doi.org/10.1002/er.3454

[8] Belkacem, Belabes, and Marius Paraschivoiu. "CFD Analysis of a Finite Linear Array of Savonius Wind Turbines." In *Journal of Physics: Conference Series*, vol. 753, no. 10, p. 102008. IOP Publishing, 2016. https://doi.org/10.1088/1742-6596/753/10/102008

[9] Mereu, Riccardo, D. Federici, G. Ferrari, Paolo Schito, and Fabio Inzoli. "Parametric numerical study of Savonius wind turbine interaction in a linear array." *Renewable Energy* 113 (2017): 1320-1332. https://doi.org/10.1016/j.renene.2017.06.094

[10] Zhang, Baoshou, Baowei Song, Zhaoyong Mao, and Wenlong Tian. "A novel wake energy reuse method to optimize the layout for Savonius-type vertical axis wind turbines." *Energy* 121 (2017): 341-355. https://doi.org/10.1016/j.energy.2017.01.004

[11] Meziane, Mohamed, Elhachmi Essadiqi, Mustapha Faqir, and Mohamad Fathi Ghanameh. "CFD Study of Unsteady Flow Through Savonius Wind Turbine Clusters." *International Journal of Renewable Energy Research (IJRER)* 9, no. 2 (2019): 657-666.

[12] Shaheen, Mohammed, and Shaaban Abdallah. "Development of efficient vertical axis wind turbine clustered farms." *Renewable and Sustainable Energy Reviews* 63 (2016): 237-244. https://doi.org/10.1016/j.rser.2016.05.062
[13] Zheng, Y., H. L. Bai, and C. M. Chan. "Optimization of Savonius turbine clusters using an evolutionary based Genetic Algorithm." *Energy Procedia* 158 (2019): 637-642. https://doi.org/10.1016/j.egypro.2019.01.173
[14] Shaheen, Mohammed, and Shaaban Abdallah. "Efficient clusters and patterned farms for Darrieus wind turbines." *Sustainable Energy Technologies and Assessments* 19 (2017): 125-135. https://doi.org/10.1016/j.seta.2017.01.007
[15] Sun, Xiaojing, Daihai Luo, Diangui Huang, and Guoqing Wu. "Numerical study on coupling effects among multiple Savonius turbines." *Journal of Renewable and Sustainable Energy* 4, no. 5 (2012): 053107. https://doi.org/10.1063/1.4754438
[16] Golecha, Kailash, T. I. Eldho, and S. V. Prabhu. "Study on the interaction between two hydrokinetic Savonius turbines." *International Journal of Rotating Machinery* 2012 (2012). https://doi.org/10.1155/2012/581658
[17] Zakaria, Ahmad, and Mohd Shahrul Nizam Ibrahim. "Numerical Performance Evaluation of Savonius Rotors by Flow-driven and Sliding-mesh Approaches." *International Journal of Advanced Trends in Computer Science and Engineering* 8, no. 1 (2019): 57-61. https://doi.org/10.30534/ijatcse/2019/10812019
[18] Zakaria, Ahmad, and Mohd Shahrul Nizam Ibrahim. "Estimating an Optimal Multiple Savonius Wind Turbines Layout by CFD Velocity Pattern Analysis." In *Journal of Physics: Conference Series*, vol. 1300, no. 1, p. 012062. IOP Publishing, 2019. https://doi.org/10.1088/1742-6596/1300/1/012062
[19] Dobrev, Ivan, and Fawaz Massouh. "CFD and PIV investigation of unsteady flow through Savonius wind turbine." *Energy Procedia* 6 (2011): 711-720. https://doi.org/10.1016/j.egypro.2011.05.081
[20] Tian, Wenlong, Zhaoyong Mao, Baoshou Zhang, and Yanjun Li. "Shape optimization of a Savonius wind rotor with different convex and concave sides." *Renewable Energy* 117 (2018): 287-299. https://doi.org/10.1016/j.renene.2017.10.067